

Quartz crystal microbalance setup for frequency and Q -factor measurements in gaseous and liquid environments

Michael Rodahl^{a)}

Department of Applied Physics, Chalmers University of Technology & Göteborg University, S-412 96 Göteborg, Sweden

Fredrik Höök

Department of Applied Physics and Department of Biochemistry and Biophysics, Lundberg Laboratory, Chalmers University of Technology & Göteborg University, S-413 90 Göteborg, Sweden

Anatol Krozer

Department of Applied Physics, Chalmers University of Technology & Göteborg University, S-412 96 Göteborg, Sweden

Peter Brzezinski

Department of Biochemistry and Biophysics, Lundberg Laboratory, Chalmers University of Technology & Göteborg University, S-413 90 Göteborg, Sweden

Bengt Kasemo^{a)}

Department of Applied Physics, Chalmers University of Technology and Göteborg University, S-412 96 Göteborg, Sweden

(Received 21 October 1994; accepted for publication 10 March 1995)

An experimental setup has been constructed for simultaneous measurements of the frequency, the absolute Q factor, and the amplitude of oscillation of a quartz crystal microbalance (QCM). The technical solution allows operation in vacuum, air, or liquid. The crystal is driven at its resonant frequency by an oscillator that can be intermittently disconnected causing the crystal oscillation amplitude to decay exponentially. From the recorded decay curve the absolute Q factor (calculated from the decay time constant), the frequency of the freely oscillating crystal, and the amplitude of oscillation are obtained. All measurements are fully automated. One electrode of the QCM in our setup was connected to true ground which makes possible simultaneous electrochemistry. The performance is illustrated by experiments in fluids of varying viscosity (gas and liquid) and by protein adsorption *in situ*. We found, in addition to the above results, that the amplitude of oscillation is not always directly proportional to the Q factor, as the commonly used theory states. This puts limitations on the customary use of the amplitude of oscillation as a measure of the Q factor. © 1995 American Institute of Physics.

I. INTRODUCTION

The piezoelectric quartz crystal microbalance (QCM) is an ultrasensitive weighing device,¹ consisting of a thin disk of single crystal quartz, with metal electrodes deposited on each side of the disk. The crystal can be made to oscillate at its resonant frequency, f , when connected to an external driving oscillator circuit. Most often, a so-called AT-cut crystal is used where the crystal oscillates in a shear mode. The principle of operation as a balance² is that any mass added to, or removed from, the electrode(s) induces a frequency shift, Δf , related to the mass change Δm . The high inherent sensitivity (<1 ng/cm²) derives from the high resolution with which even very small frequency changes can be measured. Sauerbrey first showed¹ that in vacuum the amount of added mass to the electrodes is linearly related to the resulting shift in resonant frequency of the oscillator, i.e.,

$$\Delta m = -C\Delta f, \quad (1)$$

where C is a constant that depends only on the thickness of the quartz slab and on the intrinsic properties of the quartz (see Ref. 2 and references therein). In Eq. (1) it is assumed

that the added mass is evenly distributed over the electrode(s) and is much smaller than the weight of the quartz disk, i.e., $\Delta f/f \ll 1$. It is also assumed that the mass is rigidly attached to the electrodes, with no slip or deformation due to the oscillatory motion. For an AT-cut, 10 MHz quartz crystal, C equals 2.25 ng cm⁻² Hz⁻¹ if each side is covered by Δm (if only one side is covered $C=4.5$ ng cm⁻² Hz⁻¹). Since it is easy to measure the resonant frequency of a 10 MHz quartz crystal with an accuracy better than 0.01 Hz it is possible to measure (in vacuum) the adsorption of much less than a monolayer of hydrogen.³

Traditionally, the QCM was used in vacuum and in gaseous environments. After Nomura⁴ showed that a crystal completely immersed in liquid can also be driven to oscillate in a stable manner, it has recently become a tool in electrochemistry.⁵ Several reports have also shown that the QCM may be used as a sensor in biomedical sciences,^{6,7} and to study molecular aspects of tribology.^{8,9}

The aim of the present work was to design a QCM measurement system capable of simultaneously measuring the frequency, the absolute Q factor, and the amplitude of oscillation of the quartz crystal, in gaseous as well as liquid environments.

^{a)}Authors to whom correspondence should be addressed.

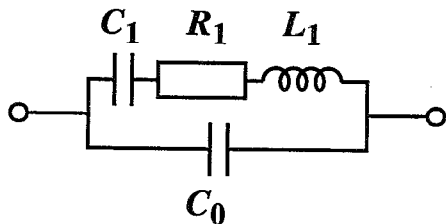


FIG. 1. The electrical equivalence of the crystal unit near principle resonance under the assumption that all undesired modes of vibration near the principle resonance are suppressed (Ref. 2).

In the following discussion it is convenient to use the dissipation factor, D , which is simply the reciprocal of the Q factor.¹⁰

$$D = \frac{1}{Q} = \frac{E_{\text{dissipated}}}{2\pi E_{\text{stored}}}, \quad (2)$$

where $E_{\text{dissipated}}$ is the energy dissipated during one period of oscillation, and E_{stored} is the energy stored in the oscillating system. A typical 10 MHz, AT-cut crystal working in a vacuum or gaseous environment has a dissipation factor in the range 10^{-6} – 10^{-4} . In the liquid phase D increases dramatically due to viscous coupling as will be shown below.

The common electrical equivalence of a quartz crystal unit near resonance is depicted in Fig. 1. Resonance occurs when the imaginary part of the total impedance for the crystal is either zero (short circuit) or infinite (open circuit) and the crystal is then said to oscillate in the series or parallel mode, respectively. From the circuit in Fig. 1 the dissipation factor can be expressed as¹⁰

$$D = \frac{R_1}{\omega L_1}, \quad (3)$$

where ω is the angular frequency at resonance and L_1 and R_1 are defined in Fig. 1.

For a simple harmonic oscillator, like the one in Fig. 1, ω is influenced by the dissipation factor according to¹¹

$$\omega = \omega_0 \sqrt{1 - D^2/2} \approx \{D \ll 1\} \approx \omega_0, \quad (4)$$

where ω_0 is the loss free resonant frequency. The maximum amplitude of oscillation, A , at resonance is given by

$$A = \frac{B}{D \sqrt{1 - D^2/4}} \approx \{D \ll 1\} \approx \frac{B}{D}, \quad (5)$$

where B is the driving force divided by the force constant.¹¹

The total loss in the QCM system is the sum of all losses in the system, i.e., the total dissipation factor, D_{tot} , can be expressed as

$$D_{\text{tot}} = \sum_i D_i, \quad (6)$$

where D_i is the dissipation factor of the i th subsystem. The energy losses in a QCM setup include, e.g., internal friction in the quartz and losses due to mounting. What is more important, for most applications, is that an adsorbed film also can dissipate energy. If the film slips on the electrode, fric-

tional energy is dissipated and D can in principle be used to infer the coefficient of friction between the adsorbed film and the electrode.^{8,9} Further, if the film is viscous, energy is also dissipated due to the oscillatory motion induced *within* the film. Consequently, if the dissipation factor can be measured with sufficient accuracy, additional information can be obtained about the viscosity and/or the slip of the adsorbed film. In a liquid, where adsorption occurs on the electrode surface, the influence of the adsorbed layer on D is superimposed on the liquid's effect on the dissipation factor. The viscoelastic coupling between the crystal and the liquid can be modified by an adsorbed monolayer of, for example, proteins, and thereby offer means of examining liquid-phase reactions at the monolayer level.¹²

In studies with overlayers (two- and three-dimensional) several investigators noted that changes in the dissipation factor may be related to changes in film structure.^{8,9,11,13,14} In these studies the dissipation factor was measured by gauging the amplitude of oscillation, i.e., the peak-to-peak value of the output signal from the oscillator, which is inversely proportional to the dissipation factor according to Eq. (5). This method is relatively simple but suffers from some drawbacks: (i) It requires that the driving force is constant, i.e., the feedback circuit in the oscillator has to be linear. (ii) It cannot be used together with automatic gain control: When a crystal is immersed in a liquid, it is commonly observed that it oscillates in a stable manner only in a very narrow drive voltage window.^{15,16} In order to ensure that this criterion is met, a common remedy is to employ an automatic gain control which matches the drive voltage to the load of the crystal.^{15,16} (iii) It does not give an absolute value of the dissipation factor and therefore calibration runs are necessary. These drawbacks are avoided using the method presented below.

Instead of using the output amplitude from the oscillator, our approach is based on the decay method used by Spencer and Smith in 1966 to study the defect concentration in natural quartz.¹⁷ The method is based on the fact that when the driving power to a simple oscillator is switched off at $t=0$, the amplitude of oscillation, A , decays as an exponentially damped sinusoid.¹⁰

$$A(t) = A_0 e^{-t/\tau} \sin(\omega t + \varphi) + \text{constant}, \quad t \geq 0, \quad (7)$$

where τ is the decay time constant, φ is the phase, and the constant is the dc offset. The decay constant is related to D_{tot} by

$$D_{\text{tot}} = \frac{2}{\omega \tau}. \quad (8)$$

By recording the amplitude of oscillation as a function of time and fitting the recorded curve to Eq. (7), τ and ω can be determined. The dissipation factor can then be calculated from Eq. (8). Below we describe the experimental solution in detail (patent pending), and demonstrate its capability by a few experimental results.

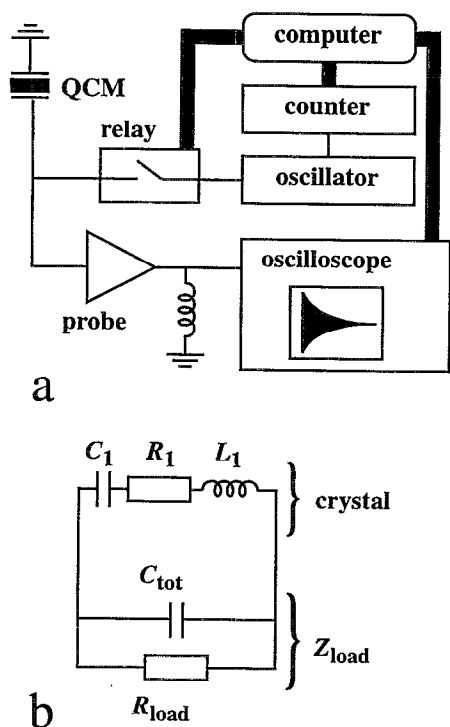


FIG. 2. (a) The experimental setup for ω and D measurements using the decay method. A measurement of the frequency and the dissipation factor of the QCM involves the following steps: (i) The computer triggers the relay to close and thereby the oscillator starts driving the QCM. (ii) A lag period of 20 ms is used to let the crystal settle in a stable oscillation. (iii) The computer simultaneously triggers the relay to open and the oscilloscope to record a decay curve. (iv) The recorded decay curve is fetched from the oscilloscope by the computer which performs a least-square fit of the wave form to the theoretical curve [Eq. (7)] using the Levenberg–Marquardt method (Ref. 20). When a frequency counter was used to measure the resonant frequency, a 1 s frequency counter measuring time was inserted before step (iii). (b) The equivalent circuit of the crystal with its load when the relay is open.

II. EXPERIMENTAL SETUP

The experimental setup is shown schematically in Fig. 2. We have modified the original setup of Spencer and Smith¹⁷ to allow full automation of the measurements, with simultaneous determination of the crystal's amplitude of oscillation, its resonant frequency, and the dissipation factor as calculated from the decay time constant [cf. Eqs. (7) and (8)]. Further, the crystal is part of an oscillator network, which reduces the need of the expensive high precision frequency generator used by Spencer and Smith. It also ensures that the crystal is always optimally driven at its resonant frequency, even if the resonant frequency changes during the course of the experiment. The latter is particularly important in measurements of adsorption isotherms and slow phase transitions, which sometimes could require runs for up to several hours or even days.

We used AT-cut quartz crystals with resonant frequencies of $10 \text{ MHz} \pm 30 \text{ kHz}$ (Quartz Pro Instruments AB, Stockholm, Sweden). One electrode of the crystal was grounded and the other was connected to the driver oscillator, via a mercury wetted relay (Clare, MSS-2). This type of relay was used to avoid bouncing at opening and closing ($\sim 1 \text{ ns}$ set-

ting time). Stable crystal oscillation was obtained within 20 ms after the relay closed. The schematics of the oscillator used for crystal operation in the gas phase or in vacuum has been published elsewhere (see Ref. 18). The schematics of the oscillator used for measurements in the liquid phase has kindly been given to us by Kanazawa and is outlined in Ref. 19. Both oscillators drive the crystal in the series mode.

The resonant frequency of the crystal with the oscillator connected, was measured with a frequency counter (Philips PM 6680). The counter was controlled by a computer via a GPIB interface. A Burr–Brown 3553 buffer amplifier was used as a probe and was connected between the crystal and the relay. The computer controlled the relay using a DA converter and fetched the recorded decay curve from the oscilloscope (LeCroy, 9450 A) using a GPIB interface. The curve was then fitted to Eq. 7 employing the Levenberg–Marquardt method.²⁰ From this fit the amplitude of oscillation, the decay time constant, and the resonant frequency of the decaying crystal were obtained.

When the relay opens there is an electrical potential (dc offset) over the crystal electrodes which is the oscillator drive voltage at this time. This causes the crystal to decay with a dc offset that can take any value between $\pm V_{\text{max}}^{\text{osc}}$, where $V_{\text{max}}^{\text{osc}}$ is the maximum output voltage from the oscillator over the crystal [approximately equal to A_0 , cf. Eq. (7)]. The oscilloscope voltage sensitivity must then be set to allow an input voltage range of $4 A_0$. A high pass filter in the form of a $3.3 \mu\text{H}$ inductor after the probe (see Fig. 2) effectively removed this dc offset in the signal from the probe. Thereby, the vertical resolution in the digitization of the decay curve was increased as the voltage range of the oscilloscope could be set to $2 A_0$ instead of $4 A_0$.

We recorded the decay curve with an oscilloscope sampling frequency, f_s , of approximately 100 kHz. Due to aliasing, the recorded signal apparently has a lower frequency, f_r , than the true signal, f , from the crystal according to

$$f_r = \frac{\text{frac}\left(\frac{f}{f_s}\right)}{\frac{1}{f} + \frac{1}{f_s}}, \quad (9)$$

where f is the crystal's resonant frequency and "frac" denotes the decimal fraction. Equation (9) is only valid if $\text{frac}(f/f_s) < 0.5$. To give a realistic example; if the crystal resonant frequency is 10.013 000 MHz and using $f_s = 100 \text{ kHz}$, the recorded signal as seen on the oscilloscope would have a frequency of 12.871 kHz. The recorded curve can hence be fitted equally well to a decaying cosine with a frequency of either 10.013 MHz or 12.871 kHz. A change in f does not result in an equally large shift in f_r . However, the difference is small. In the example above, a change in f by 1.00 Hz would result in a change in f_r by 0.99 Hz.

It is important that the probe and the relay do not appreciably dissipate energy, since this would increase the total value of the measured dissipation factor, and thereby introduce a systematic error in the determination of the total dissipation factor for the QCM. When the relay is open, the load of the crystal, Z_{load} , can be represented by a resistor, R_{load} (in

our case approximately 10^8 and $10^{11} \Omega$ for the relay and the probe, respectively) and a capacitor, C_{tot} , in parallel with the crystal, see Fig. 2. C_{tot} is the sum of all capacitors parallel to the crystal, which includes the capacitance of the probe (~ 25 pF), C_0 , and stray capacitance in the network. We estimate that the losses due to resistance in leads and contacts are negligible. The loss introduced by the measurement is the real part of Z_{load} which can be expressed as

$$\text{Re}(Z_{\text{load}}) = X_{\text{load}} = \frac{R_{\text{load}}}{1 + (\omega C_{\text{tot}} R_{\text{load}})^2}. \quad (10)$$

This loss should be compared to R_1 in Eq. (3) and therefore the additional or “parasitic” dissipation factor introduced in the measurement, D_e , is approximately

$$D_e = \frac{X_{\text{load}}}{R_1} D_0, \quad (11)$$

where D_0 is the “true” dissipation factor which would have been measured using an ideal probe with infinite resistance. The higher the value of C_{tot} the smaller is the influence of the probe, but also the smaller the voltage measured by the probe. Typically $R_1 = 10 \Omega$ and $C_0 = 5$ pF for a 10 MHz, AT-cut crystal operating in air. Neglecting stray capacitance, one can estimate X_{load} to be 3 m Ω . The parasitic dissipation contribution will in this case be of the order of 0.3%. It should also be noted that this addition to the dissipation factor is constant and canceled out if one is only interested in changes of the dissipation factor of the QCM [c.f. Eq. (6)]. In the liquid phase R_1 becomes one to two orders of magnitude larger as compared to the gas phase and the parasitic dissipation will then, relatively, be even smaller.

In our setup, the crystal was excited during approximately 20 ms for each measurement. With a minimum lag time of approximately 300 ms due to data transfer from the oscilloscope to the computer and subsequent storage onto a hard disk, the maximum sampling rate was approximately 3 Hz.

A crystal dissipates 2–150 μW during oscillation.¹⁵ This can give rise to a small temperature rise, whose magnitude depends on the heat losses. Although small, this temperature rise might be of importance in applications where it is crucial that the crystal is in equilibrium with its surroundings, e.g., during studies of phase transitions and other critical phenomena. Between measurements the crystal oscillation is in our case shut off by the computer and thereby the heating of the crystal is minimized.

In the gas and vacuum experiments the crystal was mechanically held by the electrical leads that connected the crystal with the oscillator, see Fig. 3. This arrangement exposed both electrodes to the ambient. In order to avoid short circuiting of the QCM electrodes in conductive liquids we covered one of the crystal electrodes with a thin Macor[®] (Corning) lid glued with silicone at the rim of the crystal, see Fig. 3. The crystal was then placed in a cuvette containing the liquid. Pickup noise was reduced by sealing the cuvette with a lid and enclosing it in a Faraday cage on a vibration isolation table. The electrode facing the solution was connected to true ground to further eliminate pickup noise. This is also an advantage if one wants to do simultaneous electro-

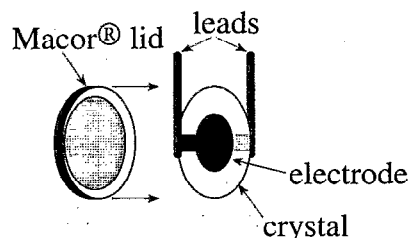


FIG. 3. In all applications, the crystal was mounted by gluing its electrodes to electrical leads with a conducting glue. In air and in vacuum both sides of the crystal were exposed to the ambient. When the crystal was submerged in liquids one side was covered with a Macor lid to avoid short circuiting of the electrodes. The lid was glued to one side of the crystal with a nonconducting glue. The leads were also covered with the nonconducting glue.

chemistry, since the grounded electrode in this case would be the working electrode in an electrochemical cell.⁵

III. PERFORMANCE

A typical measured decay curve (crosses) with a fit to Eq. (7) is shown in Fig. 4. The good fit between experiment (filled squares) and Eq. (7) (full curve) is illustrated by the magnified portion in the inset. The correlation coefficient was typically better than 0.9995 and the errors in the fitted parameters smaller than 0.5%. With a 33 MHz 386 PC the computation of the fitting parameters took approximately 2 s for the curve in Fig. 4. In air the variation over 30 measurements of the frequency was less than ± 0.1 Hz and the dissipation factor variation was less than $\pm 10^{-7}$. For each data point, only 2.4 ms of the decay curve was used to calculate the frequency and the dissipation factor. Using the same measuring time on the high precision frequency counter the variation in resonant frequency was more than ± 1 Hz.

The decay curve was not influenced by the time the relay was closed before it opened, as long as the relay was closed for at least 15 ms. The crystal did not start to oscillate before

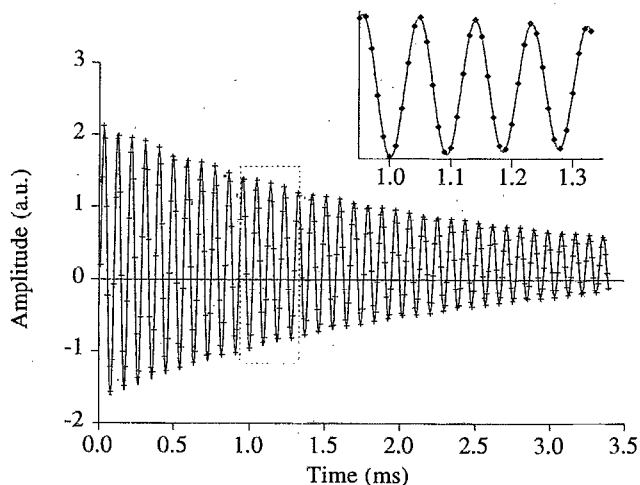


FIG. 4. A typical decay curve of a 10 MHz, AT-cut crystal measured in air. The crosses are the measured points and the solid line is the fit to Eq. (7). The inset shows a magnification of the selected part of the plot indicated by the dashed rectangle in the main figure. The apparent frequency of oscillation is lower than 10 MHz due to aliasing.

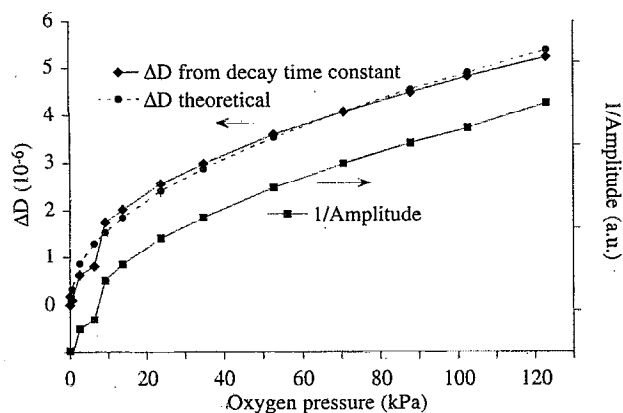


FIG. 5. Dissipation factor of a 10 MHz AT-cut crystal as a function of oxygen pressure. The filled circles and dashed curve are the theoretical curve [Eq. (12)] using $N=4$, and the diamonds represent the measured dissipation factor as calculated from the decay time constant. The inverse of the amplitude of oscillation is also shown to illustrate that the amplitude of oscillation (filled squares) and dissipation factor, mostly, are inversely proportional to each other as predicted by Eq. (5).

approximately 4 ms after the oscillator was connected. Then it took approximately 11 ms to reach full amplitude of oscillation. Because the computer could not control the timing of the opening and closing of the relay with a better accuracy than ± 2 ms, we set the relay open time to 20 ms to ensure adequate time for the crystal to settle in stable oscillation.

Two crystals with dissipation factors specified by the manufacturer were used to check our setup. Unfortunately, the dissipation factors were only quoted with 10% accuracy by the manufacturer. The results from our measurements were within this specified uncertainty.

To obtain a more precise measure of the performance, we utilized the fact that the damping of a quartz crystal as a function of gas density and viscosity, D_g , is:²¹

$$D_g = \frac{4}{\rho_q t_q} \sqrt{\frac{\rho_g \eta_g}{2\omega}} \sqrt{\frac{\omega \tau_r}{1 + (\omega \tau_r)^2} \left(\sqrt{1 + \frac{1}{(\omega \tau_r)^2}} + 1 \right)}, \quad (12)$$

where ρ_g and η_g are the gas density and viscosity, respectively. t_q is the thickness of the quartz crystal and the time τ_r is the average time required for a gas particle to lose e^{-1} of its excess momentum obtained after a collision with the moving surface. τ_r is generally expressed as $N\tau_c$, where N is an integer and τ_c is the average time between collisions in the gas phase. (τ_c is inversely proportional to the pressure, at constant temperature.) For the experiment a 10 MHz, AT-cut crystal was placed in a vacuum chamber which was pumped out over night. Then pure O_2 was introduced into the chamber and the accompanying change in dissipation factor of the crystal was recorded as a function of O_2 pressure. As shown in Fig. 5, the measured dissipation factor (upper curve, filled squares) agrees very well with Eq. (12) (filled circles, dashed curve).

In most cases, the amplitude followed the dissipation factor closely in accord with Eq. (5). An example is given in Fig. 5 (lower curve). However, we did observe deviations from perfect inverse proportionality between D and A . On

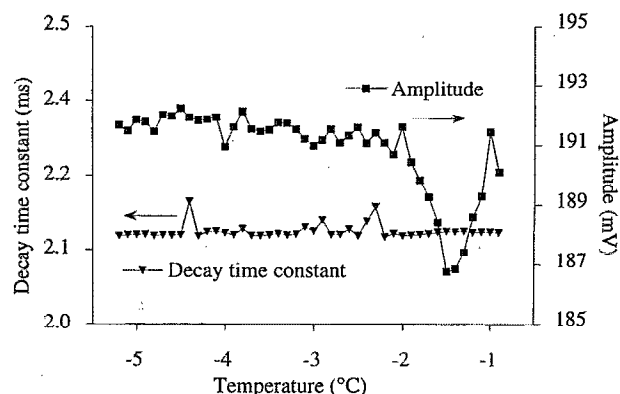


FIG. 6. A measurement of amplitude and decay time constant as a function of temperature, for a clean AT-cut, 10 MHz crystal in vacuum. This figure illustrates that the amplitude and dissipation factor do not always follow each other, i.e., a deviation from Eq. (5) is observed.

occasions the amplitude changed drastically while the dissipation factor remained constant. One example is shown in Fig. 6, where the temperature of a 10 MHz, AT-cut crystal enclosed in an evacuated chamber was scanned over 6 K at a rate of 0.02 K/min. The dip in the curve between -2 and -1 °C can be explained by coupling of two resonant modes at this temperature. If the resonant frequencies of the two resonant modes have different temperature dependencies they can reach the same value at a given temperature, in this case around -1.5 °C.²² When this happens, a so-called activity dip occurs, and the crystal is then not a simple, single oscillator and cannot be represented by the simple equivalent circuit in Fig. 1. Therefore, Eq. (5) is invalid in this case.

The resonant frequency of the decoupled, "decaying" crystal (Fig. 4), as calculated from Eq. (7), correlated very well with the stationary frequency of the driven crystal, as measured by the frequency counter. This is illustrated by a measurement where the crystal with a preadsorbed monolayer of myoglobin was oscillating in air with varying relative humidity. The change in resonant frequency was the same for the driven crystal and the freely oscillating crystal, as shown in Fig. 7. The absolute value of the resonant frequency, calculated from the decay curve, was approximately 200–800 Hz higher than that recorded by the counter, but the two frequencies followed each other closely, i.e., the frequency shifts were the same. The reason for the difference in absolute values is that the oscillating mode of the crystal changes from series to parallel mode when the relay is opened.

When measuring mass changes in the liquid phase, the simple relation in Eq. (1) breaks down and a more complex relation exists between added mass and frequency shift, due to the coupling of the crystal motion to the surrounding liquid. The details are still not fully understood but prime factors are the viscosity and density of the liquid.^{23–25}

Kanazawa and Gordon have derived an expression for the shift in resonant frequency, due to the change in viscosity and density of the surrounding medium, when the crystal is immersed from air into a liquid:²⁴

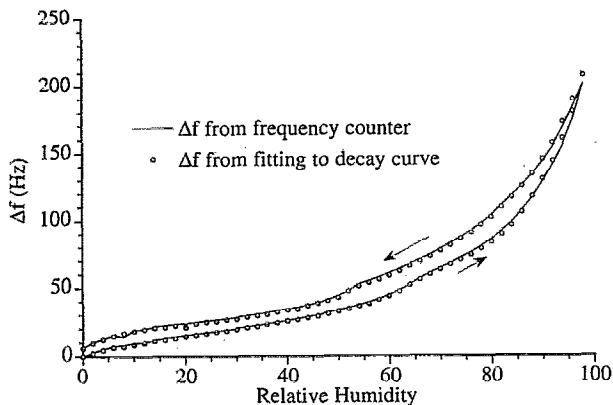


FIG. 7. A comparison between the frequency variation obtained from the fit of the decay curve to Eq. (7) and the stationary frequency measured by the frequency counter. A monolayer of myoglobin was adsorbed onto the QCM which was subsequently placed into a cell with controlled relative humidity. The relative humidity was then varied from 0% to 98% and then back to 0% (total time ~ 24 h). Note that the calculated frequency from the fit of decay curves has the same dependence on relative humidity as the frequency measured with the counter when the crystal is driven by the oscillator.

$$\Delta f = \sqrt{\frac{f_a^3}{\pi \mu_q \rho_q}} \sqrt{\eta_l \rho_l}, \quad (13)$$

where f_a is the unloaded resonant frequency of the crystal (in air), η_l and ρ_l are the absolute viscosity and density of the liquid, respectively, and μ_q and ρ_q are the elastic modulus and density of quartz, respectively.

The damping of the crystal due to the coupling of its motion to the liquid, expressed as a dissipative load, D_l , can be estimated by using Eq. (12) and noting that in a liquid $\omega\tau \ll 1$:

$$D_l = \frac{4}{\rho_q t_q} \sqrt{\frac{\rho_l \eta_l}{2\omega}}, \quad (14)$$

where ρ_l and η_l are the liquid density and viscosity, respectively. (When only one side of the crystal is contacting the liquid the damping is halved.)

When the Macor[®] lid was glued to the rim of one side of the crystal the dissipation factor increased by approximately 1.6×10^{-5} . The dissipation factor was further increased by approximately 4.7×10^{-4} when the crystal was immersed in water. Even though the overall stability was reduced in the liquid, the standard deviation from five measurements of the decaying crystal was only 2 Hz and the variation in the dissipation factor was less than 2×10^{-6} . The frequency shift caused by immersion into water at room temperature was -4.7 kHz relative to air, as measured by the decay curve. This value is reasonably close to the theoretical value of -3.5 kHz.²⁴ Measured with the oscillator connected the shift was -5.6 kHz. The difference is possibly due to different phase shifts introduced by the probe and the oscillator.²⁶

As an additional test, the dissipation factor and the resonant frequency of a 10 MHz AT-cut crystal were measured as functions of $\sqrt{\eta_l \rho_l}$, when one side of the crystal was contacting a liquid whose viscosity and density were varied. For the latter, water–glucose solutions were used with the viscosity and density values taken from Ref. 27. Figure 8 shows the

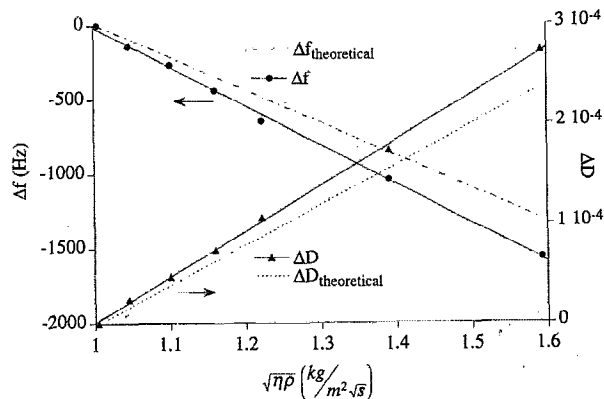


FIG. 8. Variations in dissipation factor, ΔD , and resonant frequency, Δf , as function of $\sqrt{\eta\rho}$, for an AT-cut 10 MHz crystal immersed in water–glucose mixtures. ΔD and Δf are set=0 for pure water. The solid lines are linear least-squares fits to the experiment, the dashed line is the theoretical frequency shift calculated from Eq. (13), and the dotted line is the theoretical change in ΔD according to Eq. (14).

change in resonant frequency and damping versus $\sqrt{\eta_l \rho_l}$. The measured Δf and ΔD responses were linear in $\sqrt{\eta_l \rho_l}$ as predicted by theory [cf. Eqs. (13) and (14)]. The differences in slopes between the measured and theoretical curves could be due to a surface roughness effect, since we used an unpolished crystal.²⁸ The theory does not take into account surface roughness effects and a rough crystal surface is expected to be damped more than a smooth one.²⁸

Since a prime interest of ours is to study protein interaction with surfaces, an example is given of myoglobin adsorption from a buffer solution onto a gold surface (i.e., onto the electrode of an AT-cut 10 MHz crystal). The myoglobin adsorption was followed in real time by calculating the dissipation factor and the frequency from the decay curve, see Fig. 9. At time zero in Fig. 9 myoglobin was added to the water and the solution was then stirred for a few seconds. We refrain from a detailed interpretation of these curves but they show that after addition of myoglobin and stirring, the resonant frequency decreased, indicating an apparent adsorption of myoglobin. The dissipation factor of the crystal also decreased slightly indicating that the viscous drag felt by the

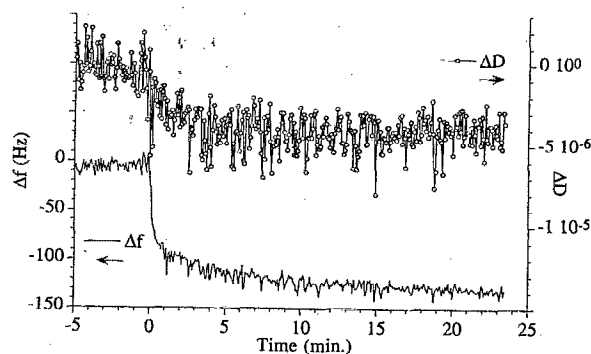


FIG. 9. Changes of resonant frequency and dissipation factor of a 10 MHz AT-cut crystal due to adsorption of hemoglobin from a buffer solution. At time zero, hemoglobin was added to the solution to a final concentration of $0.8 \mu\text{M}$ and the solution was subsequently stirred. Approximately 20 data points per minute were obtained.

crystal *decreased* due to the protein adsorption. The reason for this is not yet understood and will be subject to future studies.

As illustrated above, the method provides values of ω and D of sufficient accuracy for simultaneous evaluation of mass loads and changes in the viscous properties of the overlayer and/or in the surface-liquid coupling. The method will, in our case, be useful to measure, e.g., adsorption kinetics and adsorption isotherms of proteins in solution and, when combined with other methods such as laser spectroscopy, to measure protein functionality.

ACKNOWLEDGMENTS

We would like to thank Dr. Ken Kanazawa, IBM Almaden, for valuable discussions and suggestions about the construction of an oscillator for operation in the liquid phase. We are also grateful to Lars Hellberg and Simon Danielsson for helpful discussions on electronic matters, and to Lennart Lindberg and Guy Portnoff, Quartz Pro Instruments AB, for valuable discussions and suggestions on quartz crystals and for valuable comments on this manuscript. This work was financially supported by Swedish Research Council for Engineering Sciences (Contract No. 92-951), Swedish Biomaterials Consortium (NUTEK and NFR, Contract No. 90-02859), Swedish Micronics Program (NUTEK, Contract No. 87-03413) and by the Program for research in biotechnology at Chalmers University of Technology.

¹A. W. Czanderna, and C. Lu, in *Applications of Piezoelectric Quartz Crystal Microbalances* edited by C. Lu and A. W. Czanderna (Elsevier, Amsterdam, 1984), Vol. 7, p. 1.

²C. Lu, in Ref. 1, p. 19.

- ³B. Kasemo, and E. Törnquist, *Phys. Rev. Lett.* **44**, 1555 (1980).
- ⁴T. Nomura, and M. Okuhara, *Anal. Chim. Acta* **142**, 281 (1982).
- ⁵D. A. Buttry, in *Electroanalytical Chemistry*, edited by A. J. Bard (Dekker, New York, 1991), Vol. 17, p. 1.
- ⁶R. C. Ebersole and M. D. Ward, *J. Am. Chem. Soc.* **110**, 8623 (1988).
- ⁷Y. Okahata and H. Ebato, *Anal. Chem.* **63**, 203 (1991).
- ⁸J. Krim and R. Chiarello, *J. Vac. Sci. Technol. B* **9**, 1343 (1991).
- ⁹A. Widom and J. Krim, *Phys. Rev. B* **34**, 1403 (1986).
- ¹⁰K. L. Smith, *Electron. Wireless World* July, 51 (1986).
- ¹¹R. N. Kleiman, G. K. Kaminsky, J. D. Reppy, R. Pindak, and D. J. Bishop, *Rev. Sci. Instrum.* **56**, 2088 (1985).
- ¹²C. Barnes, C. D'Silva, J. P. Jones, and T. J. Lewis, *Sensors Actuators B* **3**, 295 (1991).
- ¹³V. M. Mecea, *Sensors Actuators A* **40**, 1 (1993).
- ¹⁴D. J. Bishop and J. D. Reppy, *Phys. Rev. Lett.* **40**, 1727 (1978).
- ¹⁵C. Barnes, *Sensors Actuators A* **29**, 59 (1991).
- ¹⁶G. C. Komplin, F. Schleifer, and W. J. Pietro, *Rev. Sci. Instrum.* **64**, 1530 (1993).
- ¹⁷W. J. Spencer and W. L. Smith, *J. Appl. Phys.* **37**, 2557 (1966).
- ¹⁸A. Krozer, Ph.D. thesis, Chalmers University of Technology, 1989.
- ¹⁹O. Melroy, K. Kanazawa, J. G. Gordon II, and D. Buttry, *Langmuir* **2**, 697 (1986).
- ²⁰W. H. Press, S. A. Teukolsky, W. T. Vetterling, and B. P. Flannery, *Numerical Recipes in Fortran* (Cambridge University Press, Cambridge, 1987).
- ²¹C. D. Stockbridge, in *Vacuum Microbalance Techniques* (Plenum, New York, 1966), Vol. 5, p. 147.
- ²²A. Ballato, and R. Tilton, *IEEE Trans. Instrum. Meas.* **IM-27**, 59 (1978).
- ²³R. Schumacher, G. Borges, and K. K. Kanazawa, *Surf. Sci.* **1163**, L621 (1985).
- ²⁴K. K. Kanazawa and J. G. Gordon III, *Anal. Chem.* **57**, 1770 (1985).
- ²⁵C. Barnes, *Sensors Actuators A* **30**, 197 (1992).
- ²⁶D. M. Soares, W. Kautek, C. Fruböse, and K. Doblhofer, *Ber. Bunsenges. Phys. Chem.* **98**, 219 (1994).
- ²⁷*CRC Handbook of Chemistry and Physics*, edited by R. C. Weast (Chemical Rubber, Boca Raton, FL, 1981-82), Vol. 62.
- ²⁸S. J. Martin, G. C. Frye, A. J. Ricco, and S. D. Senturia, *Anal. Chem.* **65**, 2910 (1993).